Large-domain integral-equation method for analysis of general 3-D electromagnetic structures

B.M. Notaroš
B.D. Popović

Indexing terms: Three-dimensional electromagnetic structures, Large-domain integral-equation analysis, Current-distribution coefficients

Abstract: A highly efficient, PC-oriented large-domain method is proposed for the analysis and CAD of a wide class of complex 3-D electromagnetic structures. The structures can be any combination of dielectric bodies, conducting surfaces and wires. The bodies are approximated by trilinear hexahedrons (distorted bricks), the surfaces by bilinear quadrilaterals (distorted rectangles) and the wires by straight-wire segments. Current distribution in the elements is approximated by high-order polynomials in local parametric co-ordinates, enabling electrically large elements. All elements can have any distributed impedance loading. In addition, the structure can have lumped loadings and generators of several kinds. The unknown current-distribution coefficients are determined by a Galerkin-type solution of a system of coupled integral equations. The principal advantage of the proposed method over existing methods is its generality combined with a comparatively small number of unknowns required for a given problem. The accuracy and versatility of the method are illustrated by a number of examples where analytical or experimental results are available.

1 Introduction

During the last decade, a number of numerical methods has been developed for the dynamic analysis of 3-D electromagnetic structures consisting of arbitrarily excited conducting and dielectric bodies of arbitrary shape. Most of these methods belongs to one of the following three basic classes:

(*a*) integral-equation frequency-domain methods [1–5]

(*b*) finite-element frequency-domain methods [6, 7]

(*c*) finite-difference time-domain methods [8, 9]

Although these classes of methods seem to be completely different, they all have a lot in common. All the methods have their advantages and deficiencies. The choice of the 'best' method usually depends on the particular problem that needs to be solved. As a rule, the methods founded on solving partial differential electromagnetic-field equations (the last two classes of methods) require supercomputers, even for the simplest 3-D open-region problems.

In this paper we concentrate on the integral-equation methods in the frequency domain. Some of these methods are based on the volume/surface formulation [1–3], and the rest on the surface/surface (pure surface) formulation [4, 5]. In the volume/surface formulation, the unknown quantities are volume electric currents inside dielectric bodies, which can be inhomogeneous, and surface electric currents over perfectly conducting surfaces. The surface/surface formulation invokes the equivalence principle, and utilises as unknown quantities equivalent electric and magnetic surface currents over boundary surfaces between the homogeneous regions of a structure. As far as the authors are informed, all the existing methods with both integral-equation formulations are basically methods of moments of subdomain type (the electromagnetic structure is approximated by many electrically small geometrical elements, with low-order basis functions for the current approximation). In the volume/surface formulation the dielectric bodies and conducting surfaces are usually modelled by cubical cells and rectangular patches, respectively, and the currents are approximated by 3-D and 2-D pulse basis functions. It is also possible to utilise thin-wall modelling of dielectric bodies, analogous to the wire-grid modelling of conducting surfaces, with 2-D rooftop basis functions defined on the wall cells [2]. For the surface/surface formulation, triangular patches with rooftop basis functions are used. As the consequence of the adopted subdomain philosophy, all these methods demand a very large number of unknown current-distribution coefficients to obtain results of satisfactory accuracy. This is the principal shortcoming of the existing methods.

This paper proposes a general, highly efficient PC-oriented method for numerical analysis of 3-D electromagnetic structures composed of dielectric bodies, conducting surfaces and wires. The dielectric bodies can be inhomogeneous and lossy. In addition to lumped loadings, the conducting surfaces and wires can have any distributed impedance loading. The structure can be excited by a plane wave, or by any number of lumped generators that can be attached to wires, surfaces and bodies. The method is founded on volume/surface integral-equation formulation in the frequency domain. Essentially, it represents a unified large-domain (less precisely, entire-domain) Galerkin-type version of the method of moments. The method can be said to be an

IEE Proceedings online no. 19982385

Paper first received 26th January and in revised form 17th June 1998

The authors are with the Department of Electrical Engineering, University of Belgrade, P.O. Box 35-54, 11120 Belgrade, Yugoslavia

extension and generalisation of the specific methods of the type [10–13]. The geometry is modelled by trilinear hexahedrons (distorted bricks), bilinear quadrilaterals (distorted rectangles) and straight-wire segments. These elements enable a simple approximation of many structures. The current in all three types of element is approximated in essentially the same way by high-order polynomials (3-D, 2-D or 1-D), enabling electrically large elements to be used. In this manner the number of unknowns is reduced greatly. The testing of the integral equations is performed by the Galerkin method.

The authors believe that, in many of its elements, the proposed method introduces significant improvements with respect to the existing methods. It appears to be the first large-domain method of such generality for the analysis of complex 3-D electromagnetic structures. A general electromagnetic code, GEM, based on the method, has been completed. Some of the results, illustrating the versatility, accuracy and efficiency of the method, are presented as examples. In all cases in which analytical or experimental results are available, excellent agreement between the results is observed.

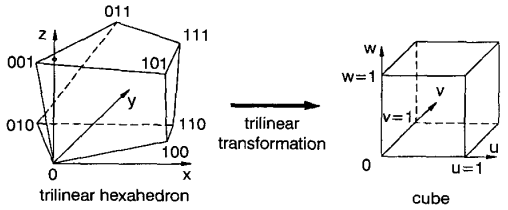

Fig.1 *Basic elements in the xyz co-ordinate system for geometrical modelling of complex electromagnetic structures and their equivalents in the uvw local parametric co-ordinate systems*

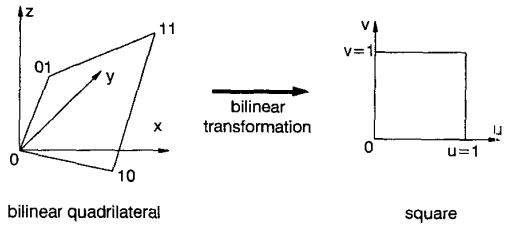

Fig.2 *Basic elements in the xyz co-ordinate system for geometrical modelling of complex electromagnetic structures and their equivalents in the uv local parametric co-ordinate systems*

2 Outline of the method

2.1 Geometrical modelling

Consider an electromagnetic structure consisting of metallic and dielectric parts of arbitrary shape. Let the structure be situated in a time-harmonic incident (impressed) field of complex electric field intensity $\mathbf{E}_i$ and angular frequency ω. As building blocks for the approximation of dielectric bodies, we adopt trilinear hexahedrons (Fig. 1). A trilinear hexahedron is defined uniquely by its eight vertices, that can be positioned in space almost arbitrarily. (Practically the only condition is that not more than four vertices are allowed to be in the same plane.) Its edges are straight, while its sides are generally curved (inflexed). Metallic surfaces are approximated by a system of infinitely thin plates in the form of bilinear quadrilaterals (Fig. 2) and the wires by straight-wire segments (Fig. 3). Since a bilinear quadrilateral is defined uniquely by its four vertices, for two trilinear hexahedrons sharing four vertices, their sides (bilinear quadrilaterals) defined by these vertices overlap exactly. Similarly, for two bilinear quadrilaterals sharing two vertices, their common edges (straight-line segments) also overlap exactly. Therefore, extremely simple exact interconnections are possible for hexahedrons, as well as for quadrilaterals. These, in fact, are generalisations of exact interconnections of wire segments (at a single point). However, this also allows exact interconnection between a side of a dielectric hexahedron and a conducting quadrilateral.

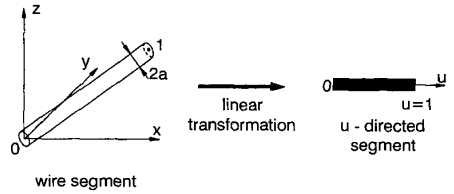

Fig.3 *Basic elements in the xyz co-ordinate system for geometrical modelling of complex electromagnetic structures and their equivalents in the u local parametric co-ordinate systems*

By introducing the parametric coordinates u, v and w ($0 \le u, v, w \le 1$), a trilinear hexahedron can be mapped onto a cube, a bilinear quadrilateral onto a square, and an arbitrarily directed wire segment onto a segment along the u-axis (Figs. 1–3). It is a simple task to show that (x, y, z) are related to (u, v, w) through the following transformations:

$$\left.\begin{aligned} x &= a_{xu}u + a_{xv}v + a_{xw}w + a_{xuv}uv \\ &\quad + a_{xuw}uw + a_{xvw}vw + a_{xuvw}uvw \\ y &= a_{yu}u + a_{yv}v + a_{yw}w + a_{yuv}uv \\ &\quad + a_{yuw}uw + a_{yvw}vw + a_{yuvw}uvw \\ z &= a_{zu}u + a_{zv}v + a_{zw}w + a_{zuv}uv \\ &\quad + a_{zuw}uw + a_{zvw}vw + a_{zuvw}uvw \end{aligned}\right\} \text{(bodies)}$$

$$\left.\begin{aligned} x &= b_{xu}u + b_{xv}v + b_{xuv}uv \\ y &= b_{yu}u + b_{yv}v + b_{yuv}uv \\ z &= b_{zu}u + b_{zv}v + b_{zuv}uv \end{aligned}\right\} \text{(plates)}$$

$$\left.\begin{aligned} x &= c_{xu}u \\ y &= c_{yu}u \\ z &= c_{zu}u \end{aligned}\right\} \text{(wires)} \qquad (1)$$

Note that the transformations are linear (for wires), bilinear (for plates) and trilinear (for bodies). The coefficients $\{a\}$, $\{b\}$ and $\{c\}$ can be expressed in terms of the co-ordinates of the element vertices (nodes), $a_{xu} = x_{100}$, $a_{xv} = x_{010}$, $a_{xw} = x_{001}$, $a_{xuv} = -x_{010} - x_{100} + x_{110}$, $a_{xuw} = -x_{001} - x_{100} + x_{101}$, $a_{xvw} = -x_{001} - x_{010} + x_{011}$, $a_{xuvw} = x_{001} + x_{010} - x_{011} + x_{100} - x_{101} - x_{110} + x_{111}$, $b_{xu} = x_{10}$, $b_{xv} = x_{01}$, $b_{xuv} = -x_{01} - x_{10} + x_{11}$, and $c_{xu} = x_1$, with analogous expressions for the co-ordinates y and z.

2.2 System of coupled integral equations for currents

The field $\mathbf{E}_i$ induces volume currents, of density $\mathbf{J}$, in the volume of dielectric bodies V_{bodies}, surface currents, of density $\mathbf{J}_s$, over the surfaces of plates S_{plates}, and line currents, of intensity I, along the generatrices of wires l_{wires} (the reduced-kernel approximation for wires). These currents, considered in a vacuum, are the sources of the scattered field

$$\mathbf{E}_s = -j\omega\mu_0 \left[\iiint_{V_{bodies}} \left(\mathbf{J} + \frac{1}{\beta_0^2} \text{div}\mathbf{J}\text{grad} \right) g\, dV \right.$$

$$+\iint_{S_{plates}}\left(\mathbf{J}_s+\frac{1}{\beta_0^2}\mathrm{div}_s\mathbf{J}_s\mathrm{grad}\right)g\,dS$$
$$+\int_{l_{wires}}\left(I\mathbf{l}_0+\frac{1}{\beta_0^2}\frac{dI}{dl}\mathrm{grad}\right)g\,dl\Bigg] \quad (2)$$

where $\mathbf{l}_0$ is the unit vector along the wire and g the Green's function

$$g=\frac{e^{-j\beta_0 R}}{4\pi R} \qquad \beta_0=\omega\sqrt{\epsilon_0\mu_0}=\frac{2\pi}{\lambda_0} \quad (3)$$

R is the distance of the field point from the source point, while β_0 and λ_0 are the free-space phase coefficient and wavelength, respectively.

The total field, $\mathbf{E}_{\text{total}}=\mathbf{E}_i+\mathbf{E}_s$, in each body satisfies the generalised local Ohm's law

$$\mathbf{E}_i+\mathbf{E}_s=\rho_e\mathbf{J} \qquad \rho_e=\frac{1}{\sigma+j\omega(\epsilon-\epsilon_0)} \quad \text{(inside bodies)} \quad (4)$$

ρ_e being the equivalent complex resistivity of the dielectric (ε and σ are the dielectric permittivity and conductivity, respectively). For plates this equation becomes

$$(\mathbf{E}_i)_{tangential}+(\mathbf{E}_s)_{tangential}=Z_s\mathbf{J}_s$$
$$Z_s=R_s+jX_s \qquad \text{(over plates)} \quad (5)$$

where Z_s is the surface impedance of the plate. Finally, along the axes of wires, we have

$$(E_i)_{axial}+(E_s)_{axial}=Z'I \qquad Z'=R'+jX'$$
$$\text{(along wires)} \quad (6)$$

where Z' is the impedance per unit length of the wire. In the case of perfectly conducting bare plates and wires, $Z_s=0$ and $Z'=0$, respectively. Eqns. 4–6, which include eqns. 2 and 3, represent a system of coupled integral equations, with unknowns $\mathbf{J}$ (inside bodies), $\mathbf{J}_s$ (over plates) and I (along wires).

2.3 High-order expansion functions

For the approximation of the components of the volume-current density vector J_u, J_v and J_w inside bodies, the components of the surface-current density vector J_{su} and J_{sv} over plates and the current intensity I along wires we adopt the power functions

$$f_{bodies}=u^i v^j w^k, \quad f_{plates}=u^i v^j, \quad f_{wires}=u^i$$
$$i=0,1,\ldots,N_u, \quad j=0,1,\ldots,N_v,$$
$$k=0,1,\ldots,N_w \quad (7)$$

where N_u, N_v and N_w are the corresponding orders of the approximation. Note that these functions are large-domain basis functions because they can be defined in electrically large elements. The larger the elements, with respect to wavelength, the higher the order of the approximation which has to be adopted (high-order expansion functions).

By combining the functions in eqn. 7, we form a set of modified power basis functions, so that each basis function satisfies the corresponding current-continuity boundary condition at a junction of elements in a geometrical model. For example, Fig. 4 shows the modified basis functions for the simplest case possible, a junction of two wires.

We adopt the testing (weighting) functions being the same as the basis functions, i.e. we use the Galerkin method. The Galerkin generalised impedances (the system matrix elements) contain several types of volume, surface and line integrals. All the integrals include the Green's function given in eqn. 3, so that the procedure of extracting the singularity must be performed for $R=0$ [11]. In accordance with the transformations in eqn. 1, the numerical integration is performed for the parametric co-ordinates, u, v and w (Figs. 1–3).

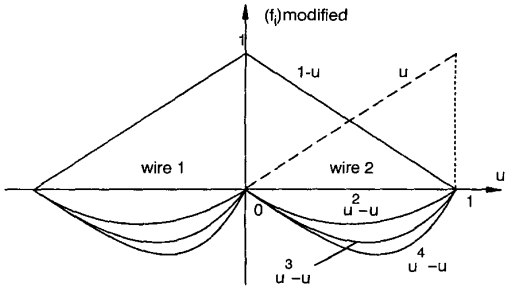

Fig. 4 *Modified power basis functions defined on two interconnected wire segments*

The excitation of transmitting antennas we model by the impressed field $\mathbf{E}_i$ due to the TEM magnetic-current frill or in the form of Dirac's delta function. Besides a standard delta generator, attached to one of the wire-segment ends (the point-delta generator) we use also a line-delta generator, which is attached to a bilinear quadrilateral edge, and a surface-delta generator associated with a trilinear hexahedron side. Lumped loads (concentrated impedances) $Z=R+jX$ are represented as current-controlled delta-generators, and incorporated into the system of equations.

The resulting system of linear algebraic equations are solved using the Gaussian elimination method giving the current-distribution coefficients, i.e. the coefficients in the expansions for $\mathbf{J}$, $\mathbf{J}_s$ and I, for a given structure. Finally, all the quantities that may be of interest for the structure analysis and design (e.g. impedances seen by generators, near field, SAR, losses in lumped and distributed resistive loadings, antenna radiation patterns, and scatterer cross-sections) are determined by post-processing of current-distribution coefficients.

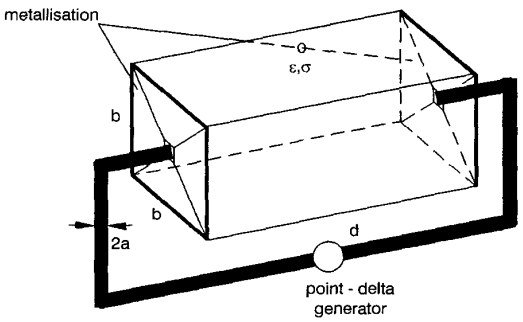

Fig. 5 *Model of resistor/capacitor connected to a low-frequency generator*

3 Results

As the first example, consider a parallelepiped made of a resistive material whose bases are metallised and connected via wire conductors to a time-harmonic voltage generator (Fig. 5). The material parameters are $\varepsilon_r=1$ and $\sigma=0.1$S/m, and the generator frequency $f=1$MHz. The metallisations are squares of edge length $b=2$mm. The distance between the metallisations is

d = 2cm and the wire radius a = 0.2mm. We assume that the metallisations and wires are perfectly conducting. Note that this structure can be regarded a realistic model of a resistor in the circuit of a low-frequency generator.

In applying the proposed method, the structure geometry is modelled by 15 elements: one dielectric body, eight plates and six wire segments (Fig. 5). The excitation is approximated by a point-delta generator. Note that the model includes also two wire-to-plate junctions at the two resistor ends. The total number of unknowns amounts to 97 and the CPU time is 4s on a PC Pentium 110MHz. The resistance seen by the generator, as obtained by the method, is $R = 2522\Omega$. We observe very good agreement with the analytical result $R_0 = d/(\sigma b^2) = 2500\Omega$.

As the next example, consider a realistic model of a capacitor in the circuit of a low-frequency generator. Let the parallelepiped in Fig. 5 be made of a perfect dielectric, of relative permittivity $\varepsilon_r = 2$ and b = 20cm ($b = 10d$). By applying the present method in the same form as in the case of a resistor model, we obtain that the susceptance seen by the generator is $B = 2.255 \cdot 10^{-4}$ S. Note that the result agrees very well with the analytical value $B_0 = \omega\varepsilon b^2/d = 2.225 \cdot 10^{-4}$ S.

Consider next a microstrip line sketched in Fig. 6. The line length is l = 50mm, the thickness of the dielectric substrate h = 2mm and the substrate relative permittivity is ε_r. The width of the upper strip is w_1 = 2mm and that of the lower strip is w_2 = 10mm. Assume that the line is lossless. The line is excited by a generator of frequency f and terminated with a purely resistive load of resistivity $R = Z_c$, where Z_c is the line characteristic impedance. The impedance Z_c is determined using a small program that has been prepared for 2-D electrostatic analysis of the line, based on a subdomain-type method-of-moments solution for the distribution of free and polarisation surface charges in the line cross-section.

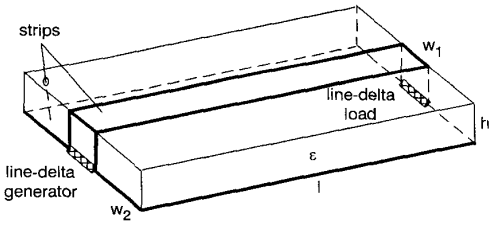

Fig. 6 *Microstrip line*

To perform a full-wave 3-D analysis of the line with the present method, we construct the geometrical model from nine elements (three dielectric bodies and six plates). The substrate is divided into three rectangular pieces, the central one of width w_1 being situated below the upper conducting strip. With this, the field variations in the vicinity of the upper strip are better approximated. A line-delta generator and a line-delta resistor are used. In Table 1 the results for the line input impedance Z and the corresponding VSWR are given for $\varepsilon_r = 1$ ($Z_c \simeq 126.5\Omega$) and $\varepsilon_r = 2$ ($Z_c \simeq 102\Omega$) and a few values of f. The frequency range is such that propagation effects along the line are present, while the radiation effects are not pronounced. Having in mind that Z_c is determined only approximately, we observe that numerical results are in a good agreement with theory (theoretically $Z = Z_c$, i.e. VSWR = 1).

Table 1: Input impedance and VSWR of the line from Fig. 6 for l = 50mm, h = 2mm, w_1 = 2mm, w_2 = 10mm and matched load

	$\varepsilon_r = 1$		$\varepsilon_r = 2$	
f, GHz	Z, Ω	VSWR	Z, Ω	VSWR
1	129.7 + j1.7	1.03	103.9 + j0.4	1.02
2	132.2 − j4.0	1.06	102.6 − j1.8	1.02
3	125.7 − j6.5	1.05	102.1 + 0.3	1.00
4	126.1 − j0.3	1.00	101.0 − j0.5	1.01
5	131.2 − j4.1	1.05	99.8 + j0.8	1.02

Sketched in Fig. 7 is a triangular printed strip monopole antenna. The substrate dimensions are h = 25.6mm, w = 21.2mm and t = 0.8mm, the diameter of the inner conductor of a coaxial line driving the antenna is d = 0.4mm and the dielectric relative permittivity is ε_r = 2.2.

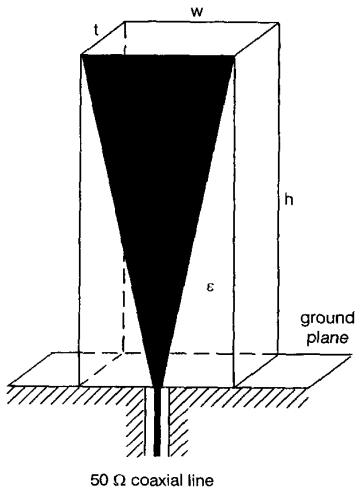

Fig. 7 *Triangular printed monopole antenna*

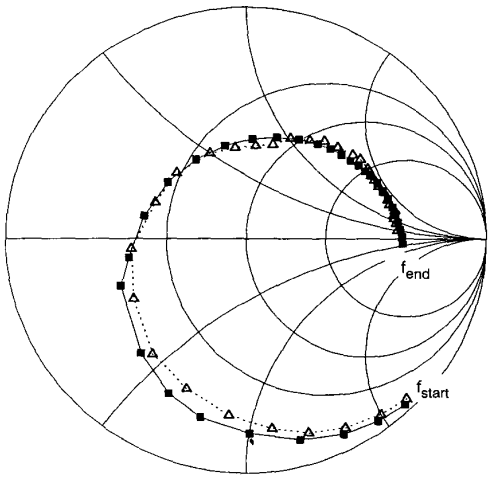

Fig. 8 *Normalised impedance of the antenna sketched in Fig. 7 for h = 25.6mm, w = 21.2mm, t = 0.8mm, ε_r = 2.2 and $Z_{reference} = 50\Omega$, against frequency $f_{start} = 1$GHz, $f_{end} \simeq 4$ GHz, step: 90 MHz ■ ■ ■ this method △ △ △ measured [14]*

The antenna is modelled with only four geometrical elements (three dielectric bodies and one plate). The perfectly conducting ground plane is taken into account by image theory. Shown in Fig. 8 is the nor-

malised antenna impedance, $z_{normalised} = Z/Z_{reference}$ ($Z_{reference} = 50\Omega$) against the generator frequency f. At the highest frequency, the number of unknowns is about 100 and the CPU time is about 30s on a PC Pentium 110MHz. We see excellent agreement between numerical and experimental results [14].

As the last example, consider a pyrimidal horn antenna sketched in Fig. 9. The dimensions of the horn (integral with its waveguide feed) are $a = 35$mm, $b = 16$mm, $c = 41$mm, $l = 145$mm, $w = 160$mm and $h = 122$mm. The length of the wire probe is 10mm and its radius is 1mm. The distance of the probe from the waveguide back (short-circuiting) wall is $d = 8$mm. This is actually a 6.0–7.0GHz, 50Ω General Radio horn. The results for the antenna impedance and the VSWR (with respect to 50Ω) against frequency, for a slightly wider range of frequencies, are given in Table 2. In the range 6–7GHz, the horn was found to have a gain of about 17dBi and a front-to-back ratio FBR ≈ 22dB.

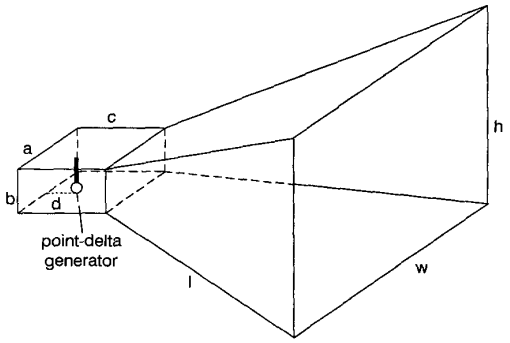

Fig. 9 *Horn antenna*

Let the horn now be covered at its opening with a 2mm thick dielectric plate (a radome) of relative permittivity $\varepsilon_r = 2.17$. The radome is assumed to lean by its four edges on the horn edges and to protrude from the horn for its thickness. It is of interest to analyse the influence of the radome on the horn impedance and radiation pattern. The impedance and VSWR for the horn with radome are shown in Table 2. It is seen that the radome does influence the horn impedance, but not considerably. The influence on the radiation pattern was found to be small, and was noticed only in the low field region.

Table 2: Impedance and VSWR (with respect to 50Ω) of the 50Ω General Radio pyramidal horn sketched in Fig. 9. The radome is added as an example, and does not exist with the original horn

	Without radome		With radome	
f, GHz	*Z*, Ω	VSWR	*Z*, Ω	VSWR
5.75	32.0 – j4.8	1.58	30.1 – j8.4	1.73
6.00	50.1 – j1.0	1.02	46.3 + j2.6	1.10
6.25	53.5 – j9.6	1.22	61.6 + j8.6	1.30
6.50	55.3 – j9.0	1.24	50.4 – j16.7	1.39
6.75	59.0 – j12.3	1.02	46.3 + j2.6	1.10
7.00	53.5 – j16.9	1.39	59.4 – j20.3	1.50
7.25	45.1 – j11.2	1.32	54.3 – j18.1	1.43

4 Conclusions

The paper presents a large-domain method for analysis of electromagnetic structures composed of dielectric bodies, conducting surfaces and wires. It is founded on a volume/surface integral equation formulation. The geometry is modelled by trilinear hexahedrons, bilinear quadrilaterals and straight-wire segments. Current distribution in the elements is approximated by high-order polynomials in local parametric co-ordinates, enabling electrically large elements. All elements can have any distributed impedance loading. The method includes appropriate models of lumped loadings and generators. The current-distribution coefficients are determined by the Galerkin method. The accuracy, versatility and stability of the method are illustrated by a number of examples where analytical or experimental results are available.

The proposed method is a highly efficient and reliable tool for the analysis and design of a wide class of complex 3-D electromagnetic structures. Its fundamental advantage over the existing methods, which are all of subdomain type, is its generality combined with the comparatively small number of unknowns required for a given problem. Although PC-oriented, the present method can of course be used on work stations and other computer systems. Parallelisation of the method is also possible.

5 References

1 SARKAR, T.K., and ARVAS, E.: 'An integral equation approach to the analysis of finite microstrip antennas: volume/surface formulation', *IEEE Trans.*, 1990, **AP–38**, (3), pp. 305–312

2 RUBIN, B.J., and DAIJAVAD, S.: 'Radiation and scattering from structures involving finite-size dielectric regions', *IEEE Trans.*, 1990, **AP–38**, (11), pp. 1863–1873

3 PARFITT, A.J., GRIFFIN, D.W., and COLE, P.H.: 'On the modeling of metal strip antennas contiguous with the edge of electrically thick finite size dielectric substrates', *IEEE Trans.*, 1992, **AP–40**, (2), pp. 134–140

4 RAO, S.M., CHA, C.-C., CRAVEY, R.L., and WILKES, D.L.: 'Electromagnetic scattering from arbitrary shaped conducting bodies coated with lossy materials of arbitrary thickness', *IEEE Trans.*, 1991, **AP–39**, (5), pp. 627–631

5 RAO, S.M., SARKAR, T.K., MIDYA, P., and DJORDJEVIĆ, A.R.: 'Electromagnetic radiation and scattering from finite conducting and dielectric structures: surface/surface formulation', *IEEE Trans.*, 1991, **AP–39**, (7), pp. 1034–1037

6 VOLAKIS, J.L., ÖZDEMIR, T., and GONG, J.: 'Hybrid finite-element methodologies for antennas and scattering', *IEEE Trans.*, 1997, **AP–45**, (3), pp. 493–507

7 ÖZDEMIR, T., and VOLAKIS, J.L.: 'Triangular prisms for edge-based vector finite element analysis of conformal antennas', *IEEE Trans.*, 1997, **AP–45**, (5), pp. 788-797

8 TAFLOVE, A.: 'Computational electromagnetics: The finite-difference time-domain method' (Artech House, Boston, 1995)

9 OKONIEWSKI, M., OKONIEWSKA, E., and STUCHLY, M.A.: 'Three-dimensional subgridding algorithm for FDTD', *IEEE Trans.*, 1997, **AP–45**, (3), pp. 422–429

10 NOTAROŠ, B.M., and POPOVIĆ, B.D.: 'General entire-domain method for analysis of dielectric scatterers', *IEE Proc.-H*, 1996, **143**, (6), pp. 498–504

11 NOTAROŠ, B.M., and POPOVIĆ, B.D.: 'Optimized entire-domain moment-method analysis of 3D dielectric scatterers', *Int. J. Numer. Model. Electron. Netw. Devices Fields*, 1997, **10**, pp. 177–192

12 POPOVIĆ, B.D., and KOLUNDŽIJA, B.M.: 'Analysis of metallic antennas and scatterers' (IEE Electromagnetic Wave Series, No.38, London, 1994)

13 NOTAROŠ, B.M., and POPOVIĆ, B.D.: 'General entire-domain Galerkin method for analysis of wire antennas in the presence of dielectric bodies', *IEE Proc. -H*, 1998, **145**, (1), pp. 13–18

14 LEBBAR, H., HIMDI, M., and DANIEL, J.P.: 'Analysis and size reduction of various printed monopoles with different shapes', *Electron. Lett.*, 1994, **30**, (21), pp. 1725–1726